RM E55L12a

NACA

RESEARCH MEMORANDUM

USE OF MEAN-SECTION BOUNDARY-LAYER PARAMETERS IN PREDICTING THREE-DIMENSIONAL TURBINE STATOR LOSSES

By Warner L. Stewart, Warren J. Whitney, and Robert Y. Wong

Lewis Flight Propulsion Laboratory
Cleveland, Ohio

NATIONAL ADVISORY COMMITTEE FOR AERONAUTICS

WASHINGTON

March 23, 1956

NATIONAL ADVISORY COMMITTEE FOR AERONAUTICS

RESEARCH MEMORANDUM

USE OF MEAN-SECTION BOUNDARY-LAYER PARAMETERS IN PREDICTING THREE-DIMENSIONAL TURBINE STATOR LOSSES

By Warner L. Stewart, Warren J. Whitney, and Robert Y. Wong

SUMMARY

A method is developed for using stator mean-section boundary-layer parameters in predicting three-dimensional stator losses. Two basic assumptions are made: (1) The momentum loss on the blade surfaces can be represented by the loss measured at the mean section; and (2) the boundary-layer momentum loss per unit area on the inner and the outer wall is approximated by the average loss on the blade surfaces.

This method is applied to a highly loaded stator. The measured mean-section boundary-layer parameters are used to obtain the variation in over-all loss total-pressure ratio, including mixing effects, for critical velocity ratios ranging from approximately 0.5 to 1.2. These predicted loss characteristics are compared with those obtained from two complete annular surveys of the stator. This comparison indicates that the theoretical stator loss total-pressure ratios based on the mean-section surveys are in very good agreement with those obtained from the annular surveys.

Although the limited experimental data do not permit generalizations, it is felt that the method presented is a reasonable approach for including end-wall effects in over-all stator loss characteristics. For the stator considered herein, excellent results were obtained with this method, even though the effect of secondary flow on stator losses was not taken into account.

INTRODUCTION

One of the important aspects of the turbine research program being conducted at the NACA Lewis laboratory is the study of the fundamental nature of the losses occurring in turbomachine blade rows. Reference 1 describes these losses in terms of boundary-layer parameters and explains the use of the parameters in calculating the effects of flow nonuniformities at the exit of two-dimensional blade rows on the over-all blade

loss. An accurate estimate of the blade losses depends on a reasonably accurate determination of the boundary-layer parameters, especially the momentum thickness, just at the blade trailing edge.

A description of these fundamental boundary-layer parameters for a typical stator is presented in reference 2. The data were obtained at the blade mean section a few thousandths of an inch downstream of the trailing edge. It was assumed that the flow at the mean radius was essentially two-dimensional and that there was no appreciable radial flow of the low-energy fluids.

Because of the additional loss incurred on the inner and outer walls, the over-all loss of a stator is greater than the loss on the blade surface alone. Therefore, in order to describe accurately the performance characteristics of stators in an annulus, the end-wall effects must be included.

This report presents a method for calculating the three-dimensional stator loss for known mean-section boundary-layer parameters. The method is applied to a highly loaded stator, and the theoretical results are compared with results obtained from limited experimental annular surveys downstream of the stator. Derivation of equations for determining the three-dimensional loss characteristics from the annular-survey results is included.

SYMBOLS

A_a annulus area, sq ft

A_b blade surface area, sq ft

A_{bl} three-dimensional boundary-layer blockage area, sq ft

A_w sum of inner and outer wall areas within blade row, sq ft

$\mathscr{A}$ aspect ratio based on mean-section chord

c mean-section chord length, ft

H form factor, δ/θ

H^* form factor, δ^*/θ^*

h blade height, ft

N number of blades

n exponent used in describing boundary-layer velocity profile

p pressure, lb/sq ft

r radius, ft

s mean-section blade spacing, ft

t mean-section blade trailing-edge thickness, ft

u distance in tangential direction, ft

V absolute gas velocity, ft/sec

α absolute flow angle measured from axial direction, deg

α_s mean-section stagger angle measured from axial direction, deg

γ ratio of specific heats

δ displacement thickness, ft

δ^* displacement-thickness parameter defined as $\frac{\delta_{tot}}{s \cos \alpha_1}$

δ_{te} ratio of tangential component of trailing-edge thickness to spacing, $\frac{t}{s \cos \alpha_1}$

θ momentum thickness, ft

θ^* momentum-thickness parameter, $\frac{\theta_{tot}}{s \cos \alpha_1}$

ρ gas density, lb/cu ft

σ mean-section solidity

Subscripts:

cr conditions at Mach number of 1.0

corr corrected to mean-section quantities

fs free stream

h hub

m mean

meas measured

t tip

tot sum of suction- and pressure-surface quantities

0 station immediately upstream of turbine stator (fig. 2)

1 station immediately downstream of stator trailing edge where mean-section surveys are made

1a station slightly farther downstream of stator exit where annular surveys are made

2 station representing blade-exit conditions after mixing

3d three-dimensional

Superscript:

' total state

DESCRIPTION OF STATOR AND EXPERIMENTAL PROCEDURE

A sketch of the stator blades used in this investigation is shown in figure 1. This blade is a highly loaded free-vortex flat-back design having 62° of turning and a design exit Mach number of approximately 1.1 at the mean radius. The tip diameter is 14 inches and the hub-tip radius ratio is 0.7. The mean-radius solidity is 1.41.

The experimental data were obtained from mean-radius surveys and annular surveys of total pressure downstream of an annular cascade of these stator blades. The surveys consisted of circumferential traverses across approximately $1\frac{1}{4}$ blade spacings with a total-pressure probe that was alined with the flow angle. The probe was a single-tube hook type with a sensing element 0.010 inch wide. The mean-radius surveys were made with the probe adjusted so that the sensing element just cleared the blade trailing edge by a few thousandths of an inch in the axial direction. The annular surveys were made about 1/4 inch downstream of the trailing edge.

The blade-inlet conditions were maintained constant at 600° R and 32 inches of mercury absolute. The blade-exit critical velocity ratio was varied by adjusting the blade-exit static pressure. The surveys were made over a range of blade-exit critical velocity ratio from approximately 0.5 to 1.2. This upper limit was selected because probe

recovery problems and shock loss in the free stream make results above this limit questionable (see ref. 2). The inner- and outer-shroud static pressures at the blade exit were computed from the average of four static-pressure taps spaced 90° apart on the shrouds. These taps were located axially in the plane of the blade trailing edge and were used for both the mean-radius surveys and the annular surveys. The blade-exit free-stream critical velocity ratio was computed from the inlet total pressure and the exit static pressure. The exit static pressure was assumed to vary linearly across the radial span between the inner- and outer-shroud values.

DEVELOPMENT OF METHOD FOR DETERMINING OVER-ALL STATOR LOSS FROM MEAN-RADIUS SURVEYS

Station Nomenclature

The station nomenclature used in this development is given in figure 2.

Station 0 represents the inlet to the blade row where the inlet total pressure p_0' is assumed to be constant over the annulus.

Station 1 is a few thousandths of an inch downstream of the blade trailing edge. Nonuniformities of flow occur in the annulus at this station owing to boundary-layer growth on both the blade surfaces and the end walls and also to trailing-edge blockage. (Station 1a is discussed in a later section.)

Station 2 represents the flow condition after complete mixing has taken place. Because the flow would generally enter a rotor before this condition is met, the station is used principally to include the effect of the nonuniformities at station 1 on the stator loss characteristics.

Fundamental Assumptions

The method described herein for including the end-wall loss in computing stator over-all performance characteristics is based on two fundamental assumptions:

(1) The average momentum loss on the stator blade surfaces is represented by an effective momentum thickness occurring at the mean section. For stators having little radial secondary flow, this effective momentum thickness may be represented by the measured mean-section momentum thickness.

(2) The momentum loss per unit area on the stator inner and outer walls is represented by the average on the blade surfaces. Essentially, this amounts to the assumption that the secondary flows at the hub and tip, although causing a transport of low-momentum fluids to the suction surface and thus forming cores of high loss, do not result in a significant net increase in the momentum loss. Because this crossover of low-energy fluids would tend to keep the wall boundary layer thin, which would increase the shear stresses, it would be expected that, if anything, this assumption would yield calculated values of three-dimensional stator losses that are somewhat smaller than the actual over-all loss.

Procedure

Appendix C of reference 1 presents the derivation of the necessary equations for obtaining the over-all two-dimensional total-pressure ratio p_2'/p_0' for specified parameters at station 1. These five parameters are:

(1) Momentum-thickness parameter:

$$\theta_1^* = \left(\frac{\theta_{tot}}{s \cos \alpha}\right)_1 = \left(\frac{\theta_{tot}}{c}\right)_1 \frac{\sigma}{\cos \alpha_1} \tag{1}$$

(2) Displacement-thickness parameter:

$$\delta_1^* = \theta_1^* H_1^* \tag{2}$$

(3) Trailing-edge-thickness parameter:

$$\delta_{te} = \frac{t}{s \cos \alpha_1} \tag{3}$$

(4) Stator-exit average free-stream critical velocity ratio $(V/V_{cr})_{fs,1}$

(5) Average exit flow angle α_1

In view of basic assumption (1), $(V/V_{cr})_{fs,1}$ and α_1 at the mean section are considered representative of the average values in the annulus at the stator exit. The two boundary-layer parameters (eqs. (1) and (2)) must be modified from the two-dimensional values to include the effects of the end walls. The blade-surface area and the annulus-wall area are related to the mean-section blade geometry as follows. It is assumed that the blade configuration can be satisfactorily approximated by an equivalent two-dimensional blade of the same height having a constant

cross section, spacing, and stagger angle equal to those at the mean section of the given blade configuration. Such an equivalent blade is shown in figure 3. The blade surface area is approximated by the relation

$$A_b = 2chN$$

For certain types of blading (for example, impulse rotor blades with a high degree of turning), a closer approximation to the surface area would be required.

The wall area based on blade mean-section geometry (fig. 3) is approximated by

$$A_w = 2Nsc \cos \alpha_s$$

Thus, the ratio of the total area to blade-surface area can be expressed

$$\frac{A_b + A_w}{A_b} = 1 + \frac{\cos \alpha_s}{\sigma \mathscr{A}}$$

By use of assumption (2), equation (1) can be modified to include the additional momentum loss due to the end walls. This equation would then be

$$\theta^*_{1,3d} = \left(1 + \frac{\cos \alpha_s}{\sigma \mathscr{A}}\right)\left(\frac{\theta_{tot}}{c}\right)_{m,1} \frac{\sigma}{\cos \alpha_{m,1}} \tag{4}$$

The flow blockage due to the blade surface and wall boundary layer $\delta^*_{1,3d}$ can be related to the momentum thickness $\theta^*_{1,3d}$ by a form factor H^*. Reference 2 indicates that the form factor H^* can be satisfactorily approximated by the theoretical form factor H for a simple-power-law velocity profile having an exponent of 1/7, for the blades investigated in the reference. A curve of H as a function of critical velocity ratio is shown in figure 4. This curve was obtained from equation (B12) of reference 1. Thus, with an H determined from figure 4 and $\theta^*_{1,3d}$ calculated from equation (4), $\delta^*_{1,3d}$ can be obtained from equation (2) as

$$\delta^*_{1,3d} = H\, \theta^*_{1,3d} \tag{5}$$

The blockage due to the trailing-edge thickness, expressed as a percentage of the total flow area, would be the same for the three-dimensional concept as for the two-dimensional case. Thus,

$$\delta_{te,3d} = \frac{t}{s \cos \alpha_1} \tag{6}$$

All the necessary equations for including the wall effects are now derived for use in obtaining the over-all three-dimensional loss total-pressure ratio p_2'/p_0'. Therefore, if $(\theta_{tot}/c)_{m,1}$ is known from mean-section surveys together with $(V/V_{cr})_{fs,m,1}$ and $\alpha_{m,1}$, the loss total-pressure ratio can be computed from equation (C22) of reference 1, using the relations of equations (4) to (6).

The experimental data were used to obtain the mean-section momentum-thickness - chord ratio $(\theta_{tot}/c)_{m,1}$ in the manner described in reference 2. The quantities $\theta^*_{m,1}$ and $\delta^*_{m,1}$ were obtained by integrating the total-pressure traces across one blade pitch and using equations (17a) and (17b) of reference 1 as follows:

$$\delta^* = 1 - \int_0^1 \frac{\rho V}{\rho_{fs} V_{fs}} d\frac{u}{s} \tag{7}$$

and

$$\theta^* = 1 - \delta^* - \int_0^1 \frac{\rho V^2}{\rho_{fs} V_{fs}^2} d\frac{u}{s} \tag{8}$$

The trailing-edge term δ_{te} was omitted in equation (7) because the traces had no perceptible mass-flow void region corresponding to the trailing-edge thickness, as discussed in reference 2. It was assumed (as in ref. 1) that the static pressure and total temperature through the boundary layer were the same as in the free stream. Thus, the following relations can be employed:

$$\frac{\rho}{\rho_{fs}} = \left(\frac{p'}{p'_{fs}}\right)^{\frac{\gamma-1}{\gamma}} \tag{9}$$

and

$$\left(\frac{V}{V_{fs}}\right)^2 = \frac{1 - \left(\frac{p}{p'}\right)^{\frac{\gamma-1}{\gamma}}}{1 - \left(\frac{p}{p'_{fs}}\right)^{\frac{\gamma-1}{\gamma}}} \tag{10}$$

Once $\theta^*_{m,1}$ is known, $(\theta_{tot}/c)_{m,1}$ at the mean section can be computed from equation (1) using blade geometry and the exit flow angle $\alpha_{m,1}$. This angle $\alpha_{m,1}$ was taken as approximately design value (62.4°) for sonic and subsonic values of $(V/V_{cr})_{fs,m,1}$. For supersonic values of $(V/V_{cr})_{fs,m,1}$ the effect of expansion downstream of the stator throat was considered in obtaining $\alpha_{m,1}$ by assuming continuity and isentropic flow between the blade throat and the downstream stations.

DEVELOPMENT OF METHOD FOR OBTAINING OVER-ALL LOSS TOTAL-PRESSURE RATIO FROM ANNULAR SURVEYS

In order to compare the three-dimensional stator loss obtained from the mean-section boundary-layer parameters with the loss obtained from annular surveys, a method must be devised for computing the over-all loss total-pressure ratio p'_2/p'_0 from the annular surveys.

Station Nomenclature

The location of the stations is shown in figure 2. At station 0, two total-pressure ratios must be considered instead of just one, as previously used:

(1) A free-stream total pressure $p'_{meas,0}$ is measured in the region removed from the end-wall boundary layers.

(2) A calculated total pressure p'_0 is obtained from the weight flow, average static pressure, total temperature, and flow area. This total pressure, which includes the effect of the end-wall boundary layer, is more accurate for rating the stator, because the boundary layer up to the face of the stator should not be charged to the stator itself. From the data obtained in the test facility used for the subject investigation,

$$\frac{p'_0}{p'_{meas,0}} = 0.993 \tag{11}$$

In general, this value would depend on the configuration of the inlet ducting to the stator face.

Station 1a is about 1/4 inch downstream of the stator trailing edge (fig. 2) because the design radial variation in the trailing-edge axial

position makes a survey just at the trailing edge impracticable. At this station, the annular variation in total pressure p'_{1a} is obtained. As an example, the variation in $p'_{1a}/p'_{meas,0}$ at approximately design exit velocity is presented in figure 5. The exit flow angle α_{1a} is also measured at this station and is taken as the average value of the angles measured between the stator blade wakes.

As in the mean-radius surveys, station 2 represents the flow condition where complete mixing has taken place.

Development of Equations

With the assumption of a linear variation in static pressure from hub to tip, the radial variation in $p_{1a}/p'_{meas,0}$ can be computed. From these pressure-ratio values, the approximate radial variation in $(V/V_{cr})_{fs,1a}$ is easily obtained. Figure 6 shows the radial variation in critical velocity ratio at approximately design exit velocity.

Once the radial variation in critical velocity ratio is known for a given stator operating point, the procedure for computing the radial variation in θ^*_{1a} and δ^*_{1a} is the same as that for $\theta^*_{m,1}$ and $\delta^*_{m,1}$, discussed in the previous section, by the use of equations (7) to (10). The radial variation in θ^*_{1a} and δ^*_{1a} at approximately design exit velocity is shown in figure 7.

In order to obtain an over-all loss total-pressure ratio across the stator from the annular survey, the radial variation in θ^*_{1a} and δ^*_{1a} must be corrected to flow conditions representative of the average flow conditions in the annulus. The flow conditions at the mean section are considered herein to be representative of the average conditions. A three-dimensional value of δ^*_{1a} and θ^*_{1a} must then be obtained by means of an integration over the annulus.

The method for obtaining these three-dimensional quantities is outlined as follows. For a given radius, δ^*_{1a} is modified by the equation

$$\delta^*_{1a,corr} = \delta^*_{1a} \frac{(\rho V)_{fs,1a}}{(\rho V)_{fs,m,1a}} \tag{12}$$

where $\delta_{1a,corr}$ is then the blockage at that radius if $(V/V_{cr})_{fs,1a}$ is adjusted to $(V/V_{cr})_{fs,m,1a}$.

Now $\delta_{la,corr}$ is on a per unit height basis and is the ratio of blockage per blade to spacing, or the ratio of total blockage at that radius to the circumference. Thus, $\delta_{la,corr}$ can then be related to the three-dimensional blockage area at that radius dA_{bl} by

$$\frac{dA_{bl}}{2\pi r\ dr} = \delta^*_{la,corr} \tag{13}$$

By substituting equation (12) into (13), rearranging, and integrating,

$$A_{bl} = 2\pi \int_{r_h}^{r_t} \delta^*_{la} \frac{(\rho V)_{fs,la}}{(\rho V)_{fs,m,la}}\ r\ dr \tag{14}$$

By definition of a three-dimensional displacement-thickness parameter

$$\delta^*_{la,3d} = \frac{A_{bl}}{A_a}$$

a final integration of $\delta^*_{la,3d}$ can be obtained, using equation (14), as

$$\delta^*_{la,3d} = \frac{2\displaystyle\int_{r_h}^{r_t} \delta^*_{la} \frac{(\rho V)_{fs,la}}{(\rho V)_{fs,m,la}}\ r\ dr}{r_t^2\left[1 - \left(\frac{r_h}{r_t}\right)^2\right]} \tag{15}$$

In a similar manner it can be shown that

$$\theta^*_{la,3d} = \frac{2\displaystyle\int_{r_h}^{r_t} \theta^*_{la} \frac{(\rho V^2)_{fs,la}}{(\rho V^2)_{fs,m,la}}\ r\ dr}{r_t^2\left[1 - \left(\frac{r_h}{r_t}\right)^2\right]} \tag{16}$$

Using the mean-section values of $(V/V_{cr})_{fs,m,la}$ and $\alpha_{m,la}$ and the three-dimensional boundary-layer parameters of equations (15) and (16) ($\delta_{te,la}$ is assumed to be zero), an over-all loss total-pressure ratio $p'_2/p'_{0,meas}$ can be computed by the method of reference 1. Then,

since

$$\frac{p_2'}{p_0'} = \frac{p_2'}{p_{0,meas}'} \left(\frac{p_0'}{p_{0,meas}'} \right)^{-1} \tag{17}$$

the over-all loss total-pressure ratio for the stator p_2'/p_0' can be computed with the value of $p_0'/p_{0,meas}'$ from equation (11).

EXPERIMENTAL RESULTS

The mean-section boundary-layer characteristics measured at station 1 were used to compute the variation in over-all loss total-pressure ratio p_2'/p_0' with stator-exit free-stream critical velocity ratio. The values of the momentum-thickness parameter $\theta^*_{m,1}$ were selected from a faired curve of $\theta^*_{m,1}$ against critical velocity ratio at even values of $(V/V_{cr})_{fs,m,1}$. The stator loss total-pressure ratio computed from the mean-radius surveys are represented by the solid line in figure 8. The two points shown represent the stator loss total-pressure ratio computed from the results of the two annular surveys at station 1a. As can be seen from the figure, very good agreement was obtained in predicting the stator loss total-pressure ratio.

CONCLUDING REMARKS

This report has presented a method for using stator mean-section boundary-layer parameters in predicting three-dimensional stator losses. The results of the application of this method to a highly loaded stator are compared with the results obtained from two complete annular surveys. This comparison indicated very good agreement in predicting the over-all stator loss total-pressure ratio. Although the results cannot be generalized because of the limited amount of experimental data, it is felt that the method presented is a reasonable approach for including the end-wall loss. Although the effect of secondary flow on stator loss was not considered, this omission did not appear to cause any appreciable error in the predicted over-all stator loss.

Lewis Flight Propulsion Laboratory
National Advisory Committee for Aeronautics
Cleveland, Ohio, December 8, 1955

REFERENCES

1. Stewart, Warner L.: Analysis of Two-Dimensional Compressible-Flow Loss Characteristics Downstream of Turbomachine Blade Rows in Terms of Basic Boundary-Layer Characteristics. NACA TN 3515, 1955.

2. Whitney, Warren J., Stewart, Warner L., and Miser, James W.: Experimental Investigation of Turbine Stator-Blade-Outlet Boundary-Layer Characteristics Compared with Theoretical Results. NACA RM E55K24, 1956.

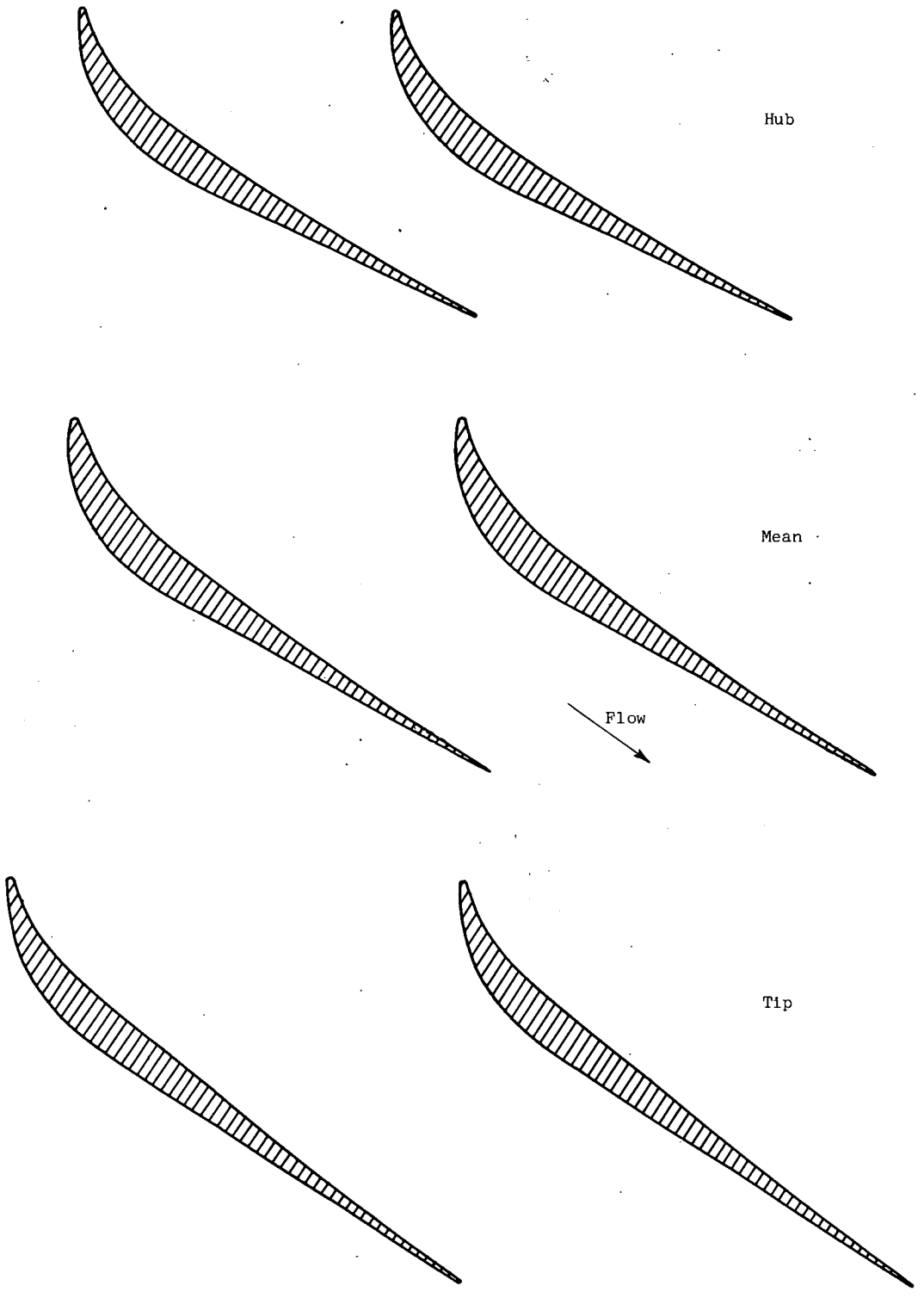

Figure 1. - Stator blade passages and profiles.

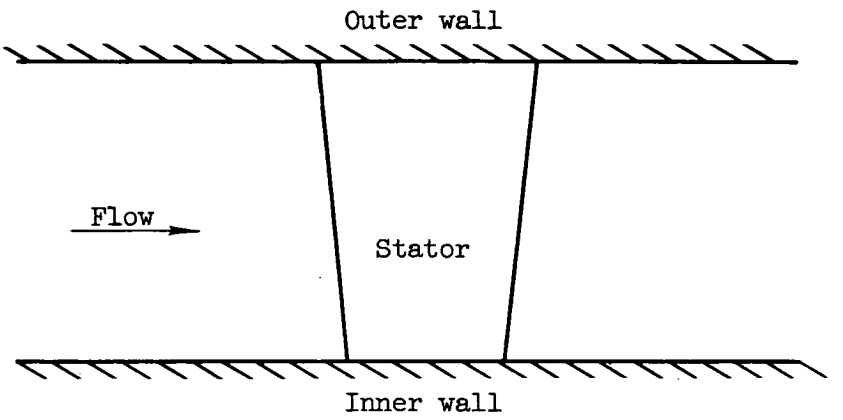

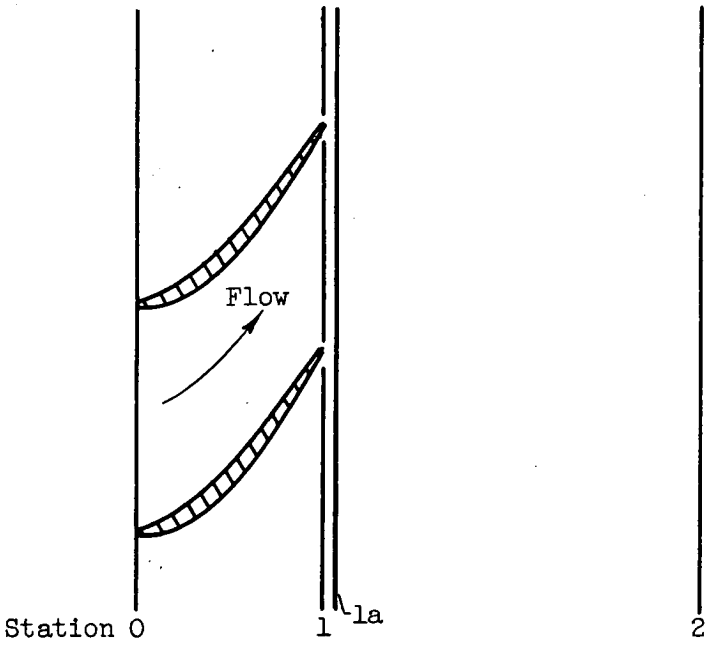

Figure 2. - Station nomenclature.

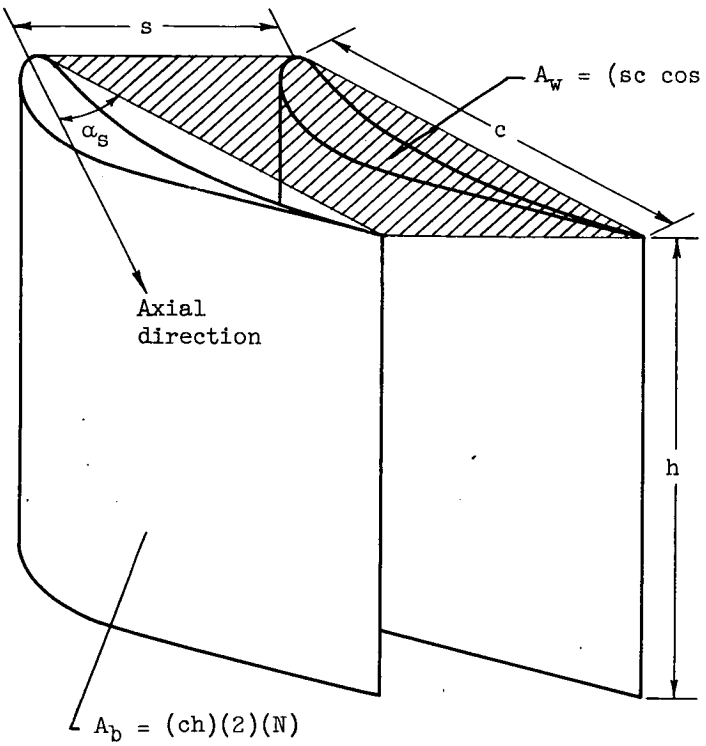

Figure 3. - Schematic of equivalent blade indicating method used to include effect of wall area in blade-loss characteristics.

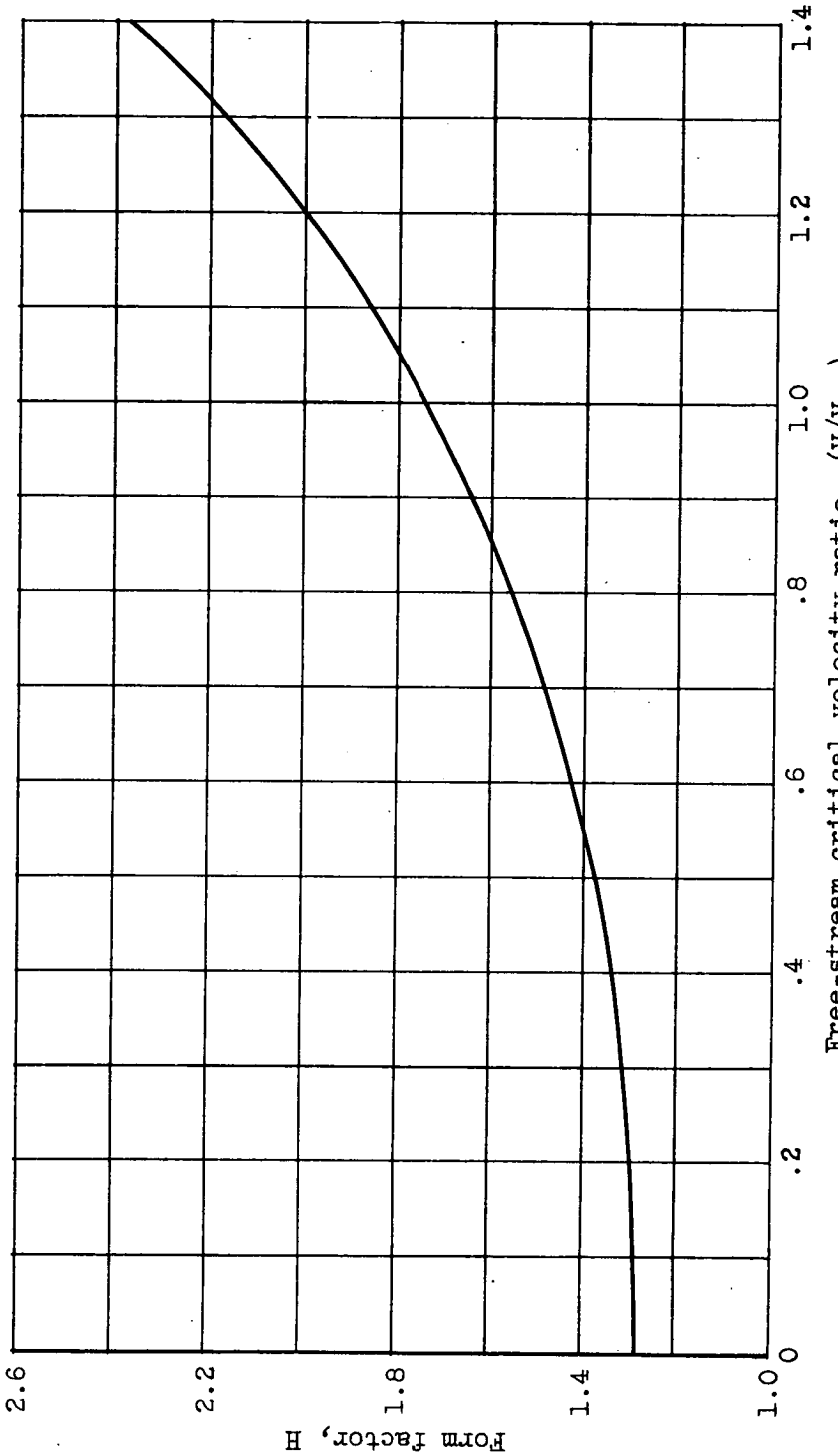

Figure 4. - Variation of form factor H with free-stream critical velocity ratio for simple-power-law velocity profile having exponent n of 1/7.

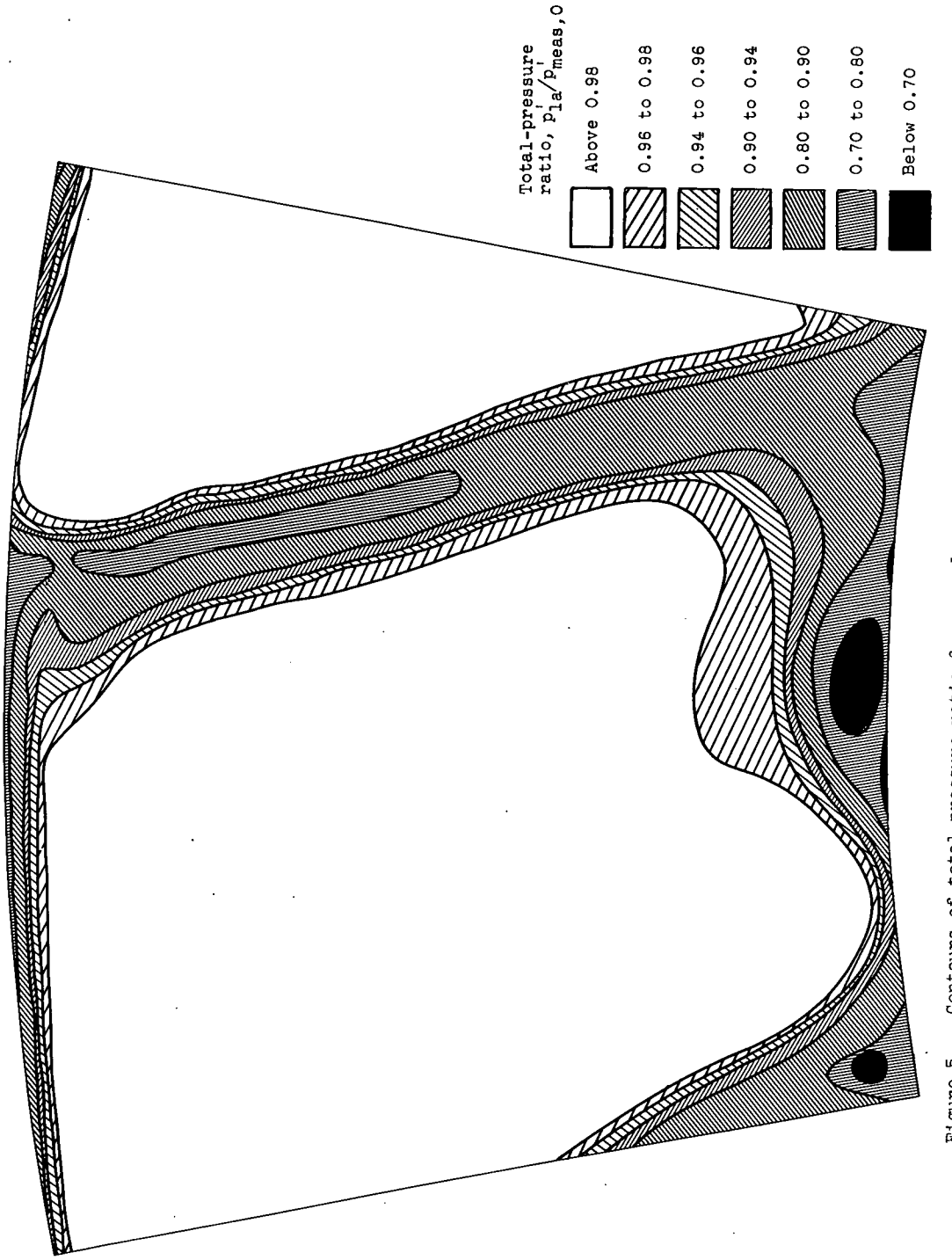

Figure 5. - Contours of total-pressure ratio from annular surveys at station 1a at approximately design stator-exit velocity. Section corresponds to about $1\frac{1}{4}$ stator passages.

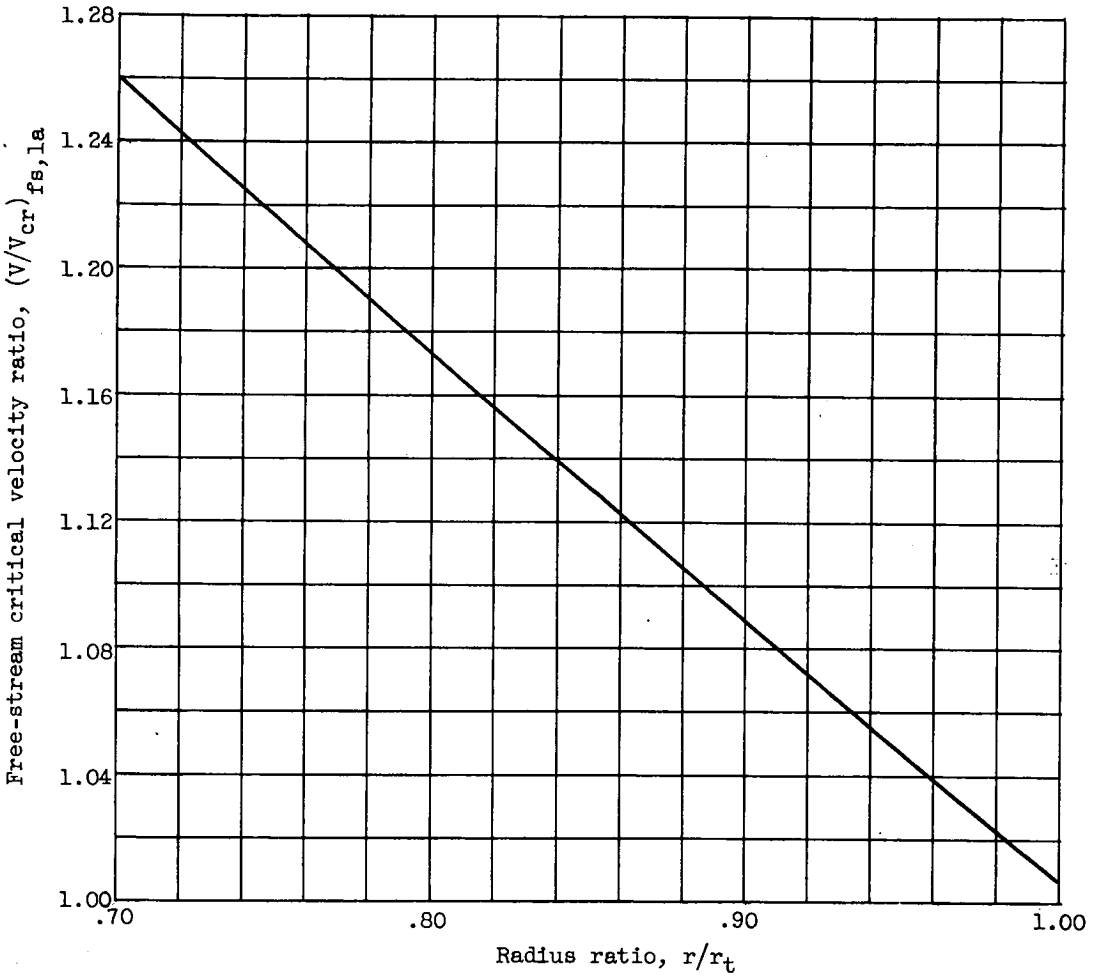

Figure 6. - Radial variation in free-stream critical velocity ratio based on annular surveys at approximately design exit velocity.

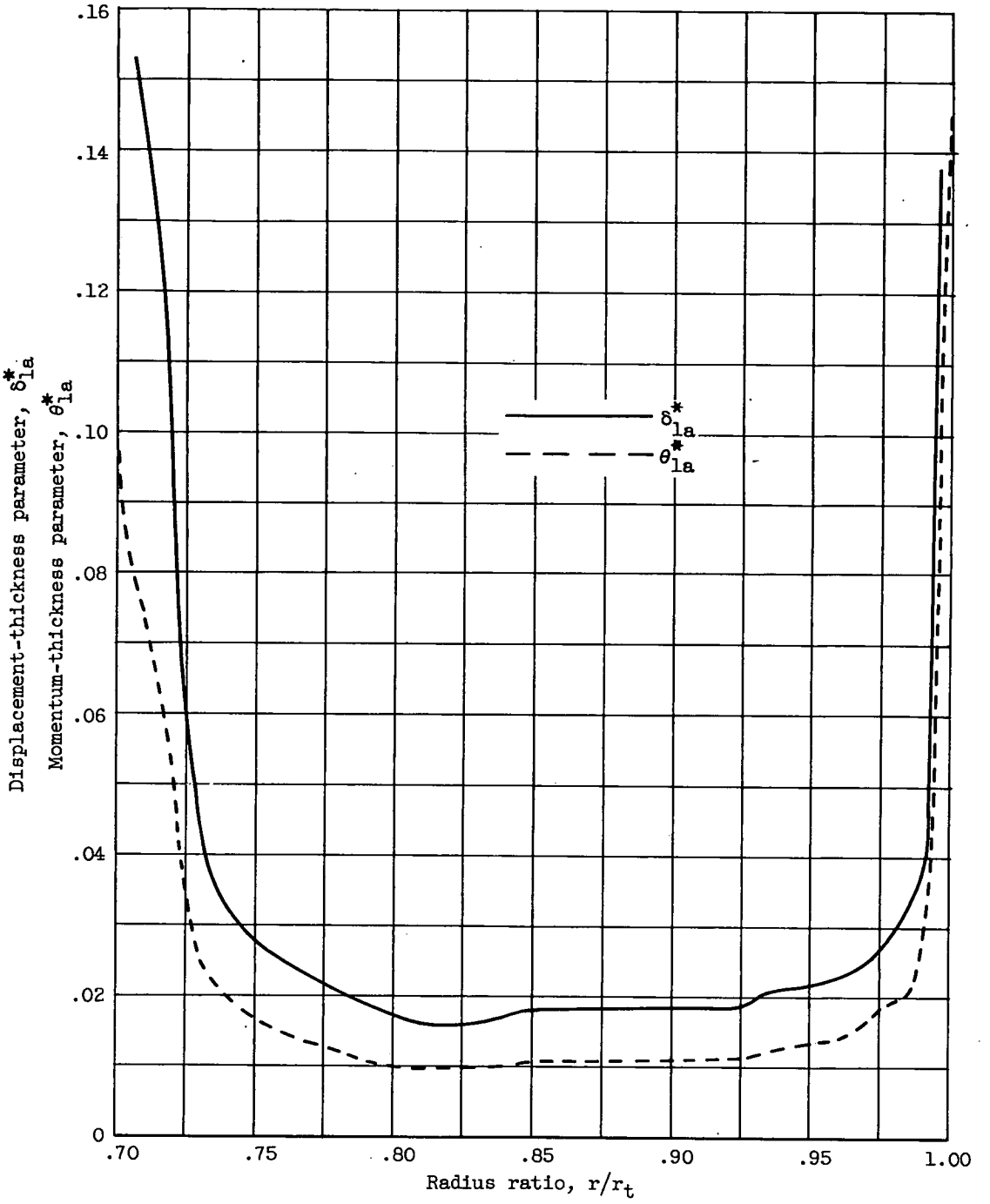

Figure 7. - Radial variation of displacement-thickness and momentum-thickness parameters based on annular surveys at approximately design exit velocity.

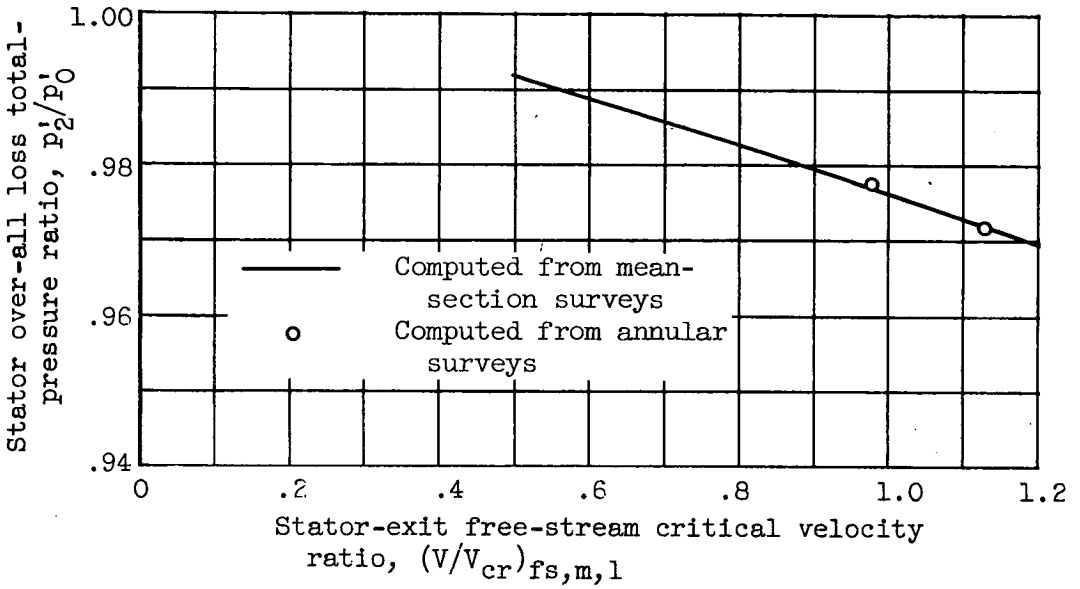

Figure 8. - Comparison of over-all loss total-pressure ratios computed from mean-section surveys and from annular surveys.